JOURNAL OF CATALYSIS 25, 407–415 (1972)

Small Angle X-Ray Scattering Investigation of Platinum Metal Dispersions on Alumina Catalysts

T. E. WHYTE, JR., P. W. KIRKLIN, R. W. GOULD,* AND HEINZ HEINEMANN

Mobil Research and Development Corporation, Research Department, Paulsboro, New Jersey 08066

Received October 21, 1971

The metal particle size diameters and particle size distributions of platinum supported on alumina catalysts have been investigated using small angle X-ray scattering techniques. The interfering background scattering from the micropores of the alumina support was eliminated by adsorption of small concentrations of CH_2I_2 and C_4H_9I, organic liquids of electron density similar to that of the alumina. Although CH_2I_2 is twice as effective as C_4H_9I in reducing the pore scattering from the η-alumina support, care must be exercised to prevent an excess of organic material which will cause unwanted scattering. The primary parameters derived from the scattering of X-rays by the platinum crystallites are R_G, the Guinier radius, and R_P, the Porod radius. These radii are expressed as the ratio of moments of a distribution which is related to σ^2 and μ, the variance and geometric mean, respectively, of a log-normal particle size distribution function. Using this simple procedure, we find that both the mean particle diameter and the particle size distribution of an aged 0.62 wt % Pt on alumina catalyst have shifted to larger sizes. In the experimental intensity curves of a 0.35 wt % Pt catalyst and that of the fresh 0.62 wt % Pt catalyst, shoulders are observed that are more or less pronounced. This behavior indicates interparticle scattering effects, suggesting the presence of small clusters of platinum particles approximately 200 Å in diameter before any agglomeration has ocurred.

INTRODUCTION

While numerous investigations (*1–6*) have reported studies of dispersed metal systems, characterization of dilute concentrations of platinum on acidic oxide supports is an especially difficult problem. There have been many qualitative studies (*7–12*) of the catalytic activity of supported platinum metal, but few have been able to quantify or follow, in detail, the changes which occur under exposure to high temperature, pressure, and other typical reaction conditions. These investigations have generally relied on the following techniques for characterizing metallic dispersion and crystallite size: X-ray line broadening, electron microscopy, gas phase chemisorption, and small angle X-ray scattering. In the case of some metals and metal alloys, e.g., Ni, Co, and Fe, magnetic measurements have been applied.

The application of X-ray line broadening techniques (*13–15*) to the specific problem of platinum dispersed on alumina, a catalytic system, which is of critical interest to those in the petroleum industry, is complicated because the major diffraction lines of alumina coincide with those of platinum. Also effects due to size distributions which may modify the breadth and shape of a diffraction line must also be taken into account. Therefore, if one is extremely careful and allows correction for the degree of indeterminancy attached

* University of Florida, Gainesville, FL 32001.

to the shape and size distribution factors, an absolute accuracy not exceeding 25 to 50% may be obtained by X-ray line broadening (*16*) for particles larger than 35 Å.

Electron microscopy techniques (*3*, *17*) have been perfected such that resolving powers of 5–10 Å are attainable. One can determine distribution of particle sizes, average particle sizes, and the tendency for metal crystallites to cluster. If the particles are large, the shape and crystal form may also be obtained. However, the extremely small sample area viewed in electron microscopy introduces severe problems of sampling. One must examine numerous areas and count thousands of particles to obtain the distribution of particle sizes. Despite these limitations, electron microscopy represents a real aid in characterizing supported metal systems.

The most thoroughly investigated method (*6*, *18–24*), to date for measuring platinum dispersion on acidic bases, especially for very low concentrations of metal, i.e., ≤ 1 wt %, is gas phase chemisorption. The most frequently used techniques are hydrogen and CO chemisorption (*22*) and the hydrogen–oxygen titration method (*23*). The latter technique is quite simple and, in principle, the most sensitive. Oxygen is first chemisorbed on the platinum surface and then displaced by means of hydrogen at room temperature. The water produced is scavenged by the alumina support. Background corrections for adsorption of hydrogen on the alumina support are negligible. The rather tedious preparation of the catalyst surface, necessary for the hydrogen or CO chemisorption method, is not required. Since two hydrogen atoms react to form water and one hydrogen is finally adsorbed, one should be able to measure the loss of three hydrogen atoms from the gas phase for every surface platinum atom, which had previously adsorbed oxygen. Therefore, the hydrogen–oxygen titration method provides a threefold increase in sensitivity over normal hydrogen and CO chemisorption.

There have been only a few reports (*25*, *26*) in the literature concerning the application of small angle X-ray scattering techniques (SAXS) to the characterization of platinum on alumina supports. The lack of work in this area is due in part to complications encountered in applying the method to catalytic systems. In fact, as Guinier (*27*) points out, ". . . in the early days of X-ray diffraction, scattering close to the primary beam was a nuisance to be disposed of with a large beam trap." One major practical difficulty with SAXS investigation of supported metals is that many of the catalyst supports have scattering centers approximately the same size as the metal crystallites. Since the platinum particles are located in the micropores themselves, interference between the two scattering systems is observed. Therefore, these holes cannot be treated as simply background radiation; and this scattering must be eliminated to observe the SAXS characteristics of the metallic constituent alone.

Earlier Gunn (*28*) demonstrated that such scattering from micropores of a silica–alumina cracking catalyst could be eliminated by sorption of high electron density liquids. Other investigators (*29*) found that high pressure sintering techniques (at 100 kbar or more) reduce the holes on alumina to a size where no SAXS is observed.

Harkness *et al* (*30*) and Gould (*31*) recently showed that the SAXS parameters (R_G, the Guinier radius; and R_P, the Porod radius) can be expressed as ratios of moments of a distribution which could be related in turn to the parameters σ^2 and μ, the variance and the geometric mean, respectively, characterizing a log normal particle size distribution. The combination of a simple effective technique to reduce background scattering from the micropores of the support without extensive pretreatment, together with a statistical method of treating the experimental parameters, makes the application of SAXS an excellent tool for characterization of supported metal catalysts.

In this study we have investigated the effects of several sorbed pore maskants in reducing SAXS from the micropores of

alumina catalysts. The treated catalysts were then examined by SAXS techniques. Using the Guinier and Porod radii to derive the variance (σ^2) and geometric mean (μ), characterizing a log-normal distribution function, we obtained mean metal particle diameters and platinum particle size distributions of fresh and aged Pt/Al_2O_3 catalysts.

Theory

The intensity of scattered X-rays is related to the size and shape of the scattering particles* and to the heterogeneity in electron density. This may be expressed as

$$I(s) = (\rho - \rho_0)^2 |\Sigma(s)|^2, \quad (1)$$

where s = scatter angle, 2θ (radians), divided by the X-ray wavelength (Å), i.e., $s = 2\theta/\lambda \approx \sin 2\theta/\lambda$;

ρ, ρ_0 = electron density of particle and continuous medium, respectively.

The form factor $\Sigma(s)$ is a function of the scattering angles summed over the dimensions of the particle. These are developed by Fourier analysis which transforms size and shape parameters into angular scattering parameters. For a sphere of radius r the form function is (*32*):

$$\Sigma(s) = \frac{4\pi}{3} r^3 \cdot 3\left[\frac{\sin(2\pi rs) - (2\pi rs)\cos(2\pi rs)}{(2\pi rs)^3}\right], \quad (2)$$
$$= V\Phi$$

where V = particle volume.

$$\Phi = 3\,\frac{\sin(2\pi rs) - (2\pi rs)\cos(2\pi rs)}{(2\pi rs)^3}.$$

Therefore Eq. (1), for spheres, can be written in the form:

$$I(s) = \Delta\rho^2 V^2 \Phi^2.$$

Guinier and Fournet (*33*) have shown that near the origin Φ^2 can be approximated by an exponential:

$$I(s) \approx \Delta\rho^2 V^2 \exp\left(-\frac{4\pi^2 r^2 s^2}{5}\right). \quad (3)$$

At large values of s, Porod (*34*) has shown that:

$$\lim_{s\to\infty} I(s) = \frac{\Delta\rho^2}{8\pi^3 s^4} \cdot 4\pi r^2 = \frac{\Delta\rho^2}{8\pi^3 s^4} \cdot A, \quad (4)$$

where A = the surface area of the scattering sphere. Porod has also shown that the integral intensity is related to the particle volume by:

$$\int_0^\infty 4\pi s^2 I(s) ds = \Delta\rho^2 V. \quad (5)$$

If the spheres vary in size, i.e., there is a distribution of particle radii, then the expressions involving the radius, e.g., V^2, V, and A are average values, i.e., $\langle V^2\rangle$, $\langle V\rangle$, $\langle A\rangle$. The SAXS intensity relationships can then be used to obtain information on the distribution of particle sizes.

Log-Normal Distribution Theory

It has long been accepted in small particle statistics that their sizes are often distributed log-normally. This distribution of particle radii r can be represented by:

$$P(r) = \frac{1}{\sqrt{2\pi}\, r \ln\sigma} \cdot \exp -\left(\frac{\ln r - \ln\mu}{\sqrt{2}\ln\sigma}\right)^2, \quad (6)$$

where μ = the geometric mean of the distribution;

σ = the square root of the variance of the distribution.

If two independent properties of the distribution can be determined, then in principle, the two variables of the distribution, i.e., μ and σ, can be determined. A useful property of a log-normal distribution (which is not generally true for a normal distribution) is that if the variable, in this case r, is distributed log-normally, so are the moments of r; i.e., r^n. In other words, the average value of the nth moment can be determined by:

* To be more precise, scattering center. We use the term scattering particle throughout to denote any electron density discontinuity with the continuous, nonscattering matrix.

$$\langle r^n \rangle = \int_0^\infty r^n P(r)\, dr. \tag{7}$$

Therefore, if two moments of the log-normal distribution can be determined experimentally, the parameters, μ and σ, can be determined.

SAXS Particle Size Distribution

In Eqs. (3), (4), and (5) for a distribution of particle radii:

$$\langle V^2 \rangle = \left(\frac{4\pi}{3}\right)^2 \langle r^6 \rangle, \tag{8}$$

$$\langle A \rangle = 4\pi \langle r^2 \rangle, \tag{9}$$

$$\langle V \rangle = \frac{4\pi}{3} \langle r^3 \rangle. \tag{10}$$

It should be noted, however, that the expressions derived thus far for SAXS intensities have been derived for a point-shaped X-ray beam. Since the Kratky (*36*) SAXS camera collimation system, used in this work, produces a line-shaped X-ray beam, these expressions are slightly modified. If the SAXS intensity with a line-shaped X-ray beam is denoted $\underline{I}(s)$, then the SAXS intensity relationships (3), (4), and (5) become (*35*):

$$\underline{I}(s) \approx \frac{8\sqrt{5\pi}}{9} \Delta\rho^2 \langle r^5 \rangle \exp - \frac{4\pi^2 R_G{}^2 s^2}{5}, \tag{11}$$

$$\lim_{s \to \infty} \underline{I}(s) = \frac{\Delta\rho^2}{16\pi^2 s^3} \langle A \rangle, \tag{12}$$

$$\int_0^\infty 2\pi s \cdot \underline{I}(s)\, ds = \Delta\rho^2 \langle V \rangle, \tag{13}$$

where R_G is the spherical radius of gyration, denoted the Guinier radius. R_G can be determined from the square root of the slope of the ln $I(s^2)$ SAXS curve at small values of s (*30*, *35*) and is given by:

$$R_G = \langle r^7 \rangle / \langle r^5 \rangle. \tag{14}$$

By combining Eqs. (12) and (13) with the definitions (9) and (10), another moment of the spherical radius, known as the Porod radius, can be determined without determining the absolute X-ray intensity or calculating $\Delta\rho^2$ (*30*):

$$R_P = \frac{3 \int_0^\infty 2\pi s \underline{I}(s)\, ds}{\lim_{s \to \infty} 16\pi^2 s^3 \underline{I}(s)} = \frac{3\Delta\rho^2 \langle V \rangle}{\Delta\rho^2 \langle A \rangle} \tag{15}$$

$$= \frac{\langle r^3 \rangle}{\langle r^2 \rangle}.$$

From Eqs. (6) and (7),

$$\langle r^n \rangle = \exp\left(n \ln \mu + \frac{n^2}{2} \ln^2 \sigma\right). \tag{16}$$

Thus,

$$R_G = \exp(\ln \mu + 6 \ln^2 \sigma), \tag{17}$$

$$R_P = \exp(\ln \mu + 2.5 \ln^2 \sigma). \tag{18}$$

Solving these equations for μ and σ:

$$\ln \mu = \ln R_G - 1.714 \ln R_G/R_P, \tag{19}$$

$$\ln^2 \sigma = 0.286 \ln R_G/R_P. \tag{20}$$

The parameters of the log-normal distribution are now described in terms of line-shaped X-ray beam SAXS parameters.

Experimental Methods

The SAXS camera was of conventional Kratky (*36*) design with a specimen to rear slit distance of 215 mm. A front slit of 80 μ (maximum Bragg value $\approx$ 1600 Å), together with a rear slit 1.0 cm long, was employed. The scattered X-rays were mechanically scanned at a $\Delta 2\theta$/min rate of 0.8′ or 6.0′ from 2θ equal to 11′ to 1°52′. A fine focus Cu X-ray tube operated at 40 kV and 18 mA and equipped with Ni filter was used. The detection system incorporated a sealed proportional counter (xenon filled) with pulse height analyzer. Experimentally derived SAXS intensity curves including the Guinier slope and the Porod asymptote are shown in Figs. 1 and 2.

The hydrogen titration of chemisorbed oxygen, using the method of Benson and Boudart (*23*), was performed in a conventional gas volumetric apparatus equipped with high vacuum Teflon valves (Kontes) and a mercury diffusion pump. A capacitance manometer (Granville-Phillips Model 03, Series 212; 0–100 Torr Head) was attached for sensitive differential pres-

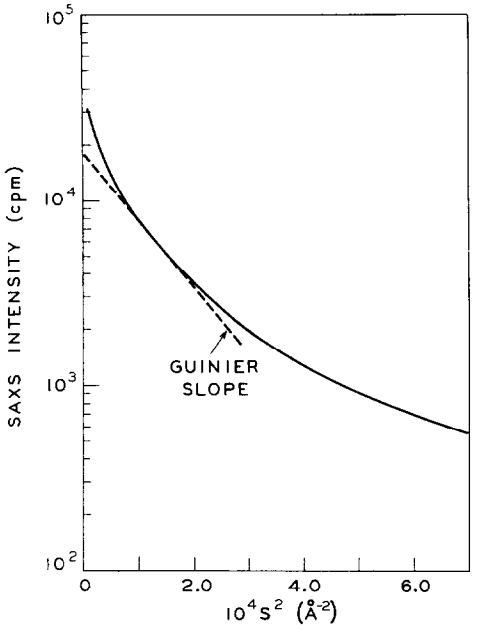

FIG. 1. SAXS Guinier curve for 0.6 wt % Pt on η-Al_2O_3.

sure measurements without mercury contamination. All gases were passed through 5A molecular sieves followed by a cooling trap containing either liquid N_2 for H_2 and He, or Dry Ice–acetone for O_2 purification.

All catalyst samples examined by SAXS (Table 1) were pretreated in H_2/16 hr/atm/950°F and then mortar ground.

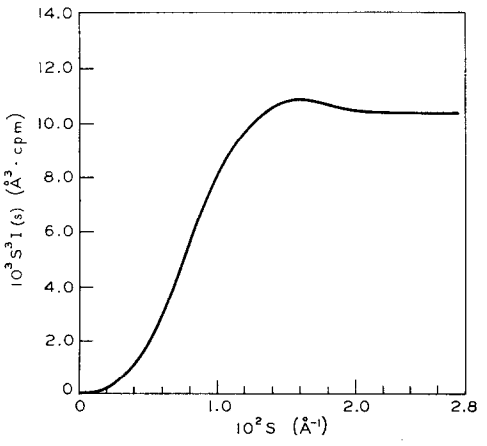

FIG. 2. SAXS Porod asymptote for 0.6 wt % Pt on η-Al_2O_3.

TABLE 1
CATALYST CHARACTERISTICS

Catalysts[a]	Pt (wt %)	SA (m^2/g)[b]	Time on-stream (months)	Carbon (wt %)
η-Al_2O_3	—	234	—	<0.01
F-6 (Fresh)	0.62	205	—	<0.01
A-6[cd] (Aged)	0.62	137	22	0.04
F-3 (Fresh)	0.35	228	—	<0.01
A-3[cd] (Aged)	0.35	191	38	<0.03

[a] All catalysts were supported on η-alumina and pretreated 16 hrs/H_2/atm/950°F before examination.

[b] Surface area determined using N_2 BET method. Surface area of F-6 and F-3 before pretreatment 397 and 420 m^2/g, respectively.

[c] Catalysts, A-6 and A-3, were removed from commercial reformer after six and seven air regeneration cycles, respectively.

[d] Chloride contents of A-6 and A-3 were 0.26 and 0.11 wt %, respectively.

They were heated with the pore maskant on a hot plate for several minutes, first to expel trapped air from the pores and then to remove the excess liquid which can cause nonreproducible absorption of the scattered X-rays. The treated samples were then packed in 1.0 or 1.5 mm thin-walled glass capillaries for the SAXS examination.

RESULTS AND DISCUSSION

As noted earlier, before SAXS can be applied to metals dispersed on porous supports, the SAXS due to the electron density heterogeneity arising from the pores must be eliminated. In the Pt/Al_2O_3 system we are concerned with three heterogeneities: $\Delta\rho^2$ (pores-oxide), $\Delta\rho^2$ (metal-oxide), and $\Delta\rho^2$ (pores-metal). By filling the pores with a liquid of electron density equal to that of the oxide we should eliminate the pore-oxide scattering. SAXS due to pores inaccessible to the liquid can be mathematically eliminated by obtaining the difference in SAXS between a similarly treated oxide support (without dispersed metal) and the catalyst. Several liquids

TABLE 2
ELECTRON DENSITIES AND CuKα ABSORPTION COEFFICIENTS OF SELECTED COMPOUNDS

Compound	ρ_e[a]	$\Delta\rho_e^2$ (Al_2O_3-liq.)[b]	$\xi_{CuK\alpha}$[c]
Al_2O_3	1.23–1.76	—	9.9
Air (pores)	0	2.25	0
Platinum	8.57	50.0	—
H_2O	0.56	0.88	12
C_2H_5I	0.87	0.40	50
C_3H_7I	0.78	0.52	40
C_4H_9I	0.76	0.55	35
CH_2I_2	1.41	0.008	100

[a] $\rho_e = \Sigma Z_i \rho_m / M$, where Z_i = number of electrons in the ith atom of the compound, ρ_m = mass density, and M = molecular weight.

[b] $\Delta\rho_e^2$ (Al_2O_3-liq.) assumed average ρ_e (Al_2O_3) = 1.5.

[c] From atomic constants *in* Cullity, B. D., "Elements of X-Ray Diffraction," p. 466. Addison-Wesley, MA 1956.

that either reduce or eliminate pore scattering in Al_2O_3 are listed in Table 2 with the calculated $\Delta\rho_e^2$ (Al_2O_3-liq.) and the linear X-ray absorption coefficient. The latter constants are important since a reduction in SAXS intensity may occur independent of the $\Delta\rho^2$ change due to absorption of the scattered radiation by the liquid.

The marked effect of excess pore maskant is clearly shown in Fig. 3. Increasing the concentration of CH_2I_2 from 0.10 to 0.20 ml/g of catalyst reduces the pore scattering to a minimum. However, any increase above this level results in excessive scattering from the CH_2I_2.

The relative effectiveness in reducing scattering from the micropores of η-Al_2O_3 after treatment with C_4H_9I and CH_2I_2 is demonstrated in Fig. 4. At a detector elevation of 4.5 mm we note a 50 and 99.5% decrease in the intensity of scattered X-rays following the addition of C_4H_9I and CH_2I_2, respectively. This agrees well with the predicted values from the $\Delta\rho_e^2$ ratio of (C_4H_9I/air) and (CH_2I_2/air) in Column 3, Table 2.

The results of fitting the experimentally derived parameters from SAXS, R_G and R_P (Table 3), to a log-normal particle size distribution function are shown in Figs. 6 and 7. The mean diameter of the fresh F-6 catalyst (Table 3) has increased significantly from 28 to 46 Å. In the particle size distribution curves of the F-6 and A-6 catalysts (Fig. 6) over 80% of the platinum particle diameters of the aged 0.6 wt % Pt catalyst (A-6) are in a range between 30 and 70 Å compared to the

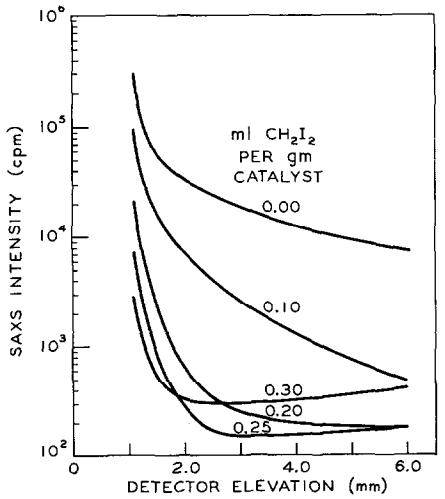

FIG. 3. Effect of CH_2I_2 concentration on SAXS of 0.35 wt % Pt on η-Al_2O_3.

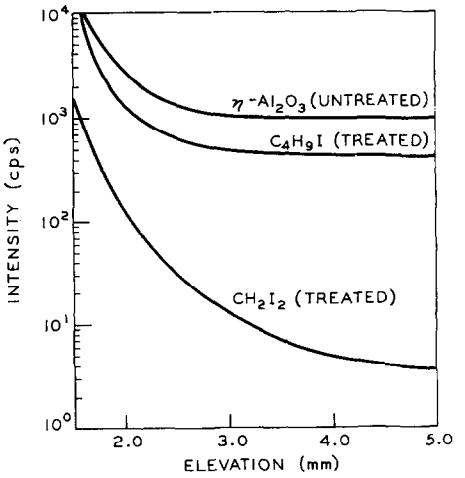

FIG. 4. Comparative effects of CH_2I_2 and C_4H_9I on SAXS of η-Al_2O_3.

TABLE 3
SMALL ANGLE X-RAY AND CHEMISORPTION RESULTS

Catalyst	Pt (wt %)	Guinier Diameter (Å) $2R_G$	Porod Diameter Å $2R_P$	Geometric mean (Å)	Diameter from chemisorption (Å)
F-6 (Fresh)	0.62	57	37	28	21
A-6 (Aged)	0.62	75	56	46	81
F-3 (Fresh)	0.35	59	41	31	20
A-3 (Aged)	0.35	64	43	32	18

fresh catalyst (F-6), which contains a 90% fraction between 10 and 50 Å in diameter.

The rather large diameter indicated for catalyst A-6, Table 3, as determined by chemisorption experiments, when compared with the values from SAXS is not surprising. The 33% loss in surface area of the alumina, Table 1, indicates some changes in the support. Any recrystallization of the alumina around the platinum particles would result in a decrease in the available metal surface area for chemisorption. This would indeed be reflected in an increase in apparent platinum diameter as determined by chemisorption.

The Guinier plots corrected for support background for all the catalysts are shown in Fig. 5. In the experimental intensity curves for catalysts, F-3 and F-6, instead of the scattering decreasing regularly from the center, shoulders are observed that are more or less pronounced. These patterns are similar to the SAXS scattering curves obtained for the hemoglobin of red blood cells. As Guinier (*32*) points out, this type of behavior is indicative of the existence of a certain degree of order in the arrangement of the particles. Thus, the platinum particles in freshly prepared samples, F-3 and F-6, although not agglomerated to any extent, may be arranged in certain patterns. This phenomenon has been reported in investigation of certain alloys (*31*). It may be treated semiquantitatively and an indication of the size of the cluster estimated. Based on the approximation of Ehrenfest (*37*), we estimate the interparticle distance as 220 Å. Although the theory is not rigorous, the observation of such maxima in the scattering curves indicates some arrangement of Pt crystallites on a freshly prepared catalyst.

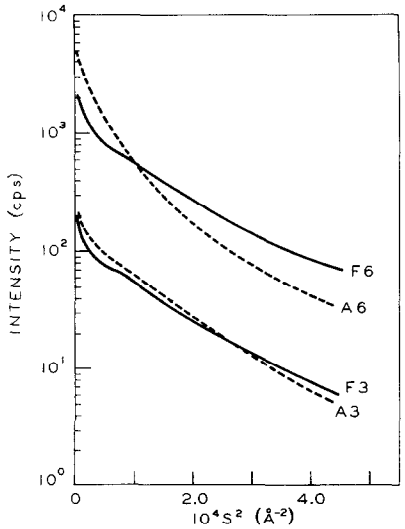

FIG. 5. Experimental small angle X-ray scattering data.

CONCLUSION

This study demonstrates that the controlled addition of organic liquids such as CH_2I_2 and C_4H_9I to platinum containing alumina catalysts eliminates the background X-ray scattering from the micropores of the support. It further shows that, although CH_2I_2 is more effective in masking the undesirable pore scattering than C_4H_9I, care must be taken such that an excess of organic sorbent will not cause SAXS scattering. The properly treated platinum catalysts can then be examined using small angle X-ray scattering tech-

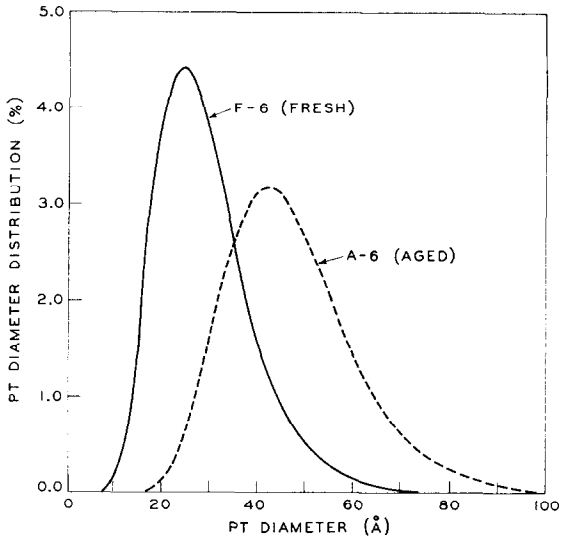

FIG. 6. SAXS determined distributions for F-6 (Fresh) and A-6 (Aged) Pt on η-Al_2O_3 catalysts.

niques. The experimentally derived Guinier radius R_G and the Porod radius R_P are characterized by a log-normal distribution function and particle size distributions realized. Using this procedure we observed a shift both in the mean metal diameter and the platinum particle size distribution of an aged Pt/Al_2O_3 catalyst to larger sizes. Evidence is also presented indicating the existence of clusters of very small platinum particles on the η-alumina support before any agglomeration has occurred. The small angle X-ray scattering method, combined with the simple masking technique and the statistical treatment of data, provides a powerful tool in the study of supported metal systems.

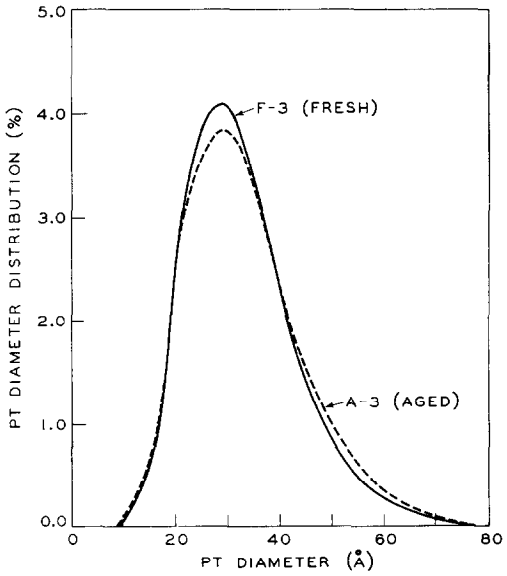

FIG. 7. SAXS determined distributions for F-3 (Fresh) and A-3 (Aged) Pt on η-Al_2O_3 catalysts.

ACKNOWLEDGMENTS

The authors thank Professor L. S. Bartell of the University of Michigan and Dr. P. B. Venuto for their valuable suggestions and comments. The technical assistance of Mr. G. R. Landolt is also gratefully acknowledged.

REFERENCES

1. SCHUIT, G. C. A., AND VAN REIJEN, L. L., *in* "Advances in Catalysis and Related Subjects" (D. D. Eley, W. G. Frankenburg, V. I. Komarewsky, and P. B. Weisz, eds.), Vol. 10, p. 242. Academic Press, New York, 1958.
2. BENESI, H. A., AND CURTIS, R. M., *J. Catal.* **10**, 328 (1968).
3. ADAMS, C. R., BENESI, H. A., CURTIS, R. M., AND MEISENHEIMER, R. G., *J. Catal.* **1**, 336 (1962).
4. MILLS, G. A., WELLER, S., AND CORNELIUS, E. B., *Actes Congr. Int. Catal., 2nd, 1960* **2**, 2221 (1961).

5. DEBYE, P., AND CHU, B., *J. Phys. Chem.* **66,** 1021 (1962).
6. ADLER, S. F., AND KEAVNEY, J. J., *J. Phys. Chem.* **64,** 208 (1960).
7. YATES, D. J. C., AND SINFELT, J. H., *J. Catal.* **14,** 182 (1969).
8. ANDERSON, J. R., AND MACDONALD, R. J., *J. Catal.* **14,** 227 (1970).
9. YATES, D. J. C., TAYLOR, W. F., AND SINFELT, J. H., *J. Phys. Chem.* **86,** 2696 (1964).
10. SINFELT, J. H., TAYLOR, W. F., AND YATES, D. J. C., *J. Phys. Chem.* **69,** 95 (1965).
11. CARTER, J. L., CUSUMANO, J. A., AND SINFELT, J. H., *J. Phys. Chem.* **70,** 2256 (1966).
12. TAYLOR, W. F., SINFELT, J. H., AND YATES, D. J. C., *J. Phys. Chem.* **69,** 3857 (1965).
13. VAN NORDSTRAND, R. A., *Anal. Chem.* **36,** 819 (1964).
14. PLANK, C. J., KOKOTAILO, G. T., AND DRAKE, L. C., Abstr. Pap. Joint Symp. Div. Petrol. Chem., Coll. and Surf. Chem., 140th ACS Meet., Chicago, Sept. 1960, p. 16-I.
15. MILLS, G. A., WELLER, S., AND CORNELIUS, E. B., *Actes Congr. Int. Catal., 2nd, 1960* **2,** 2221 (1961).
16. KLUG, H. P., AND ALEXANDER, L. E., "X-Ray Diffraction Procedures," pp. 491–538. Wiley, New York, 1954.
17. JANSEN, P. C., *Sci. Ind.* **7,** 33 (1960).
18. BENTAN, A. F., *J. Amer. Chem. Soc.* **48,** 1850 (1926).
19. BEECK, O., *in* "Advances in Catalysis and Related Subjects" (W. G. Frankenburg, V. I. Komarewsky, and E. K. Rideal, eds.), Vol. 2, p. 151. Academic Press, New York, 1950.
20. HUGHES, T. R., HOUSTON, R. J., AND SIEG, R. P., *Ind. Eng. Chem. Process Des. Develop.* **1,** 96 (1962).
21. CUSUMANO, J. A., DEMBINSKI, G. W., AND SINFELT, J. H., *J. Catal.* **5,** 471 (1966).
22. BOUDART, M., AND SPENADEL, L., *J. Phys. Chem.* **64,** 204 (1960).
23. BENSON, J. E., AND BOUDART, M., *J. Catal.* **4,** 704 (1965).
24. WILSON, G. R., AND HALL, W. K., *J. Catal.* **17,** 190 (1970).
25. SOMARJAI, G. A., dissertation, Univ. of California, Berkeley, 1960.
26. BRUMBERGER, H., "Small Angle X-ray Scattering," p. 450. Gordon and Breach, New York, 1967.
27. GUINIER, A., *Physics Today* **22,** 25 (1969).
28. GUNN, E. L., *J. Phys. Chem.* **62,** 928 (1958).
29. MONTGOMER, P. W., STRAMBERG, H., AND JURA, G., *Univ. Calif. Radiat. Lab.* **UCRL-9796** (1971).
30. HARKNESS, S. D., GOULD, R. W., AND HREN, J. J., *Phil. Mag.* **19,** 115 (1969).
31. GOULD, R. W., presented: Space Congr., 4th, Cocoa Beach, FL, 1967.
32. GUINIER, A., "X-ray Diffraction." Freeman, San Francisco, 1963.
33. GUINIER, A., AND FOURNET, G., "Small Angle Scattering of X-rays." Wiley, New York, 1955.
34. POROD, G., *Kolloid-Z.*, **124,** 83 (1951); **125,** 51, 109 (1952).
35. BAUR, R., AND GEROLD, V., *Acta Met.* **12,** 1448 (1964).
36. KRATKY, O., *Z. Elektrochem.* **58,** 49 (1954).
37. EHRENFEST, P., *Proc. Amsterdam Acad.* **17,** 1132 (1915).